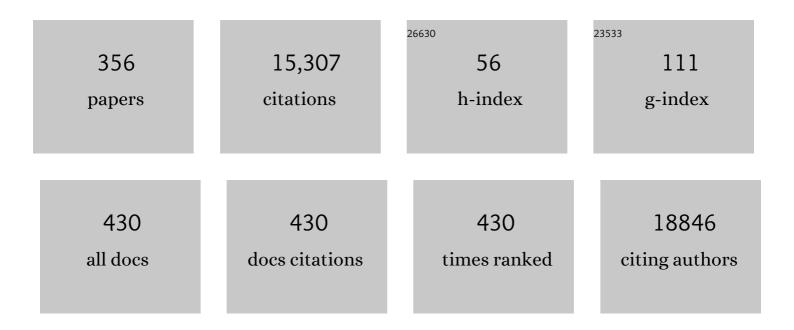
## Li Shen

## List of Publications by Year in descending order

Source: https://exaly.com/author-pdf/5001772/publications.pdf Version: 2024-02-01



#	Article	IF	CITATIONS
1	A <scp>metaâ€analysis</scp> of deep brain structural shape and asymmetry abnormalities in 2,833 individuals with schizophrenia compared with 3,929 healthy volunteers via the <scp>ENIGMA Consortium</scp> . Human Brain Mapping, 2022, 43, 352-372.	3.6	39
2	Diagnosis of obsessive-compulsive disorder via spatial similarity-aware learning and fused deep polynomial network. Medical Image Analysis, 2022, 75, 102244.	11.6	7
3	Multi-task learning based structured sparse canonical correlation analysis for brain imaging genetics. Medical Image Analysis, 2022, 76, 102297.	11.6	13
4	Genome-Wide association study of quantitative biomarkers identifies a novel locus for alzheimer's disease at 12p12.1. BMC Genomics, 2022, 23, 85.	2.8	7
5	Identifying imaging genetic associations via regional morphometricity estimation. Pacific Symposium on Biocomputing, 2022, 27, 97-108.	0.7	0
6	ldentifying highly heritable brain amyloid phenotypes through mining Alzheimer's imaging and sequencing biobank data. Pacific Symposium on Biocomputing Pacific Symposium on Biocomputing, 2022, 27, 109-120.	0.7	0
7	Sex Differences in the Metabolome of Alzheimer's Disease Progression. Frontiers in Radiology, 2022, 2,	2.0	5
8	Characterizing Heterogeneity in Neuroimaging, Cognition, Clinical Symptoms, and Genetics Among Patients With Late-Life Depression. JAMA Psychiatry, 2022, 79, 464.	11.0	47
9	Chest high-resolution computed tomography can make higher accurate stages for thoracic sarcoidosis than X-ray. BMC Pulmonary Medicine, 2022, 22, 146.	2.0	7
10	ldentifying Alzheimer's genes via brain transcriptome mapping. BMC Medical Genomics, 2022, 15, 116.	1.5	1
11	Novel Circulating Tumour Cell-Related Risk Model Indicates Prognosis and Immune Infiltration in Lung Adenocarcinoma. Journal of Immunology Research, 2022, 2022, 1-16.	2.2	5
12	Integrative analysis of summary data from GWAS and eQTL studies implicates genes differentially expressed in Alzheimer's disease. BMC Genomics, 2022, 23, .	2.8	6
13	Identify Consistent Cross-Modality Imaging Genetic Patterns via Discriminant Sparse Canonical Correlation Analysis. IEEE/ACM Transactions on Computational Biology and Bioinformatics, 2021, 18, 1549-1561.	3.0	9
14	Multi-Task Sparse Canonical Correlation Analysis with Application to Multi-Modal Brain Imaging Genetics. IEEE/ACM Transactions on Computational Biology and Bioinformatics, 2021, 18, 227-239.	3.0	25
15	A Novel Bayesian Semi-parametric Model for Learning Heritable Imaging Traits. Lecture Notes in Computer Science, 2021, 12905, 678-687.	1.3	2
16	Improved Prediction of Cognitive Outcomes via Globally Aligned Imaging Biomarker Enrichments Over Progressions. IEEE Transactions on Biomedical Engineering, 2021, 68, 3336-3346.	4.2	4
17	New pulmonary rehabilitation exercise for pulmonary fibrosis to improve the pulmonary function and quality of life of patients with idiopathic pulmonary fibrosis: a randomized control trial. Annals of Palliative Medicine, 2021, 10, 0-0.	1.2	10
18	Incidence and Outcomes of Pneumonia in Patients With HeartÂFailure. Journal of the American College of Cardiology, 2021, 77, 1961-1973.	2.8	35

#	Article	IF	CITATIONS
19	A structural enriched functional network: An application to predict brain cognitive performance. Medical Image Analysis, 2021, 71, 102026.	11.6	16
20	A new sulfated triterpene glycoside from the sea cucumber Colochirus quadrangularis, and evaluation of its antifungal, antitumor and immunomodulatory activities. Bioorganic and Medicinal Chemistry, 2021, 41, 116188.	3.0	9
21	Laryngopharyngeal pH Monitoring in Patients With Idiopathic Pulmonary Fibrosis. Frontiers in Pharmacology, 2021, 12, 724286.	3.5	2
22	lon therapy of pulmonary fibrosis by inhalation of ionic solution derived from silicate bioceramics. Bioactive Materials, 2021, 6, 3194-3206.	15.6	15
23	White Matter Integrity and Nicotine Dependence: Evaluating Vertical and Horizontal Pleiotropy. Frontiers in Neuroscience, 2021, 15, 738037.	2.8	6
24	Identifying imaging genetic associations via regional morphometricity estimation. , 2021, , .		0
25	Session Introduction: Big Data Imaging Genomics. , 2021, , .		0
26	PfAP2-EXP2, an Essential Transcription Factor for the Intraerythrocytic Development of Plasmodium falciparum. Frontiers in Cell and Developmental Biology, 2021, 9, 782293.	3.7	3
27	Genetic Influence Underlying Brain Connectivity Phenotype: A Study on Two Age-Specific Cohorts. Frontiers in Genetics, 2021, 12, 782953.	2.3	0
28	ldentifying multimodal imagingâ€driven subtypes in mild cognitive impairment using deep multiview learning. Alzheimer's and Dementia, 2021, 17, .	0.8	0
29	Brain imaging genetics: integrated analysis and machine learning. , 2021, , .		2
30	Interpretable temporal graph neural network for prognostic prediction of Alzheimer's disease using longitudinal neuroimaging data. , 2021, 2021, 1381-1384.		8
31	Hierarchical Structured Sparse Learning for Schizophrenia Identification. Neuroinformatics, 2020, 18, 43-57.	2.8	12
32	Brain Imaging Genomics: Integrated Analysis and Machine Learning. Proceedings of the IEEE, 2020, 108, 125-162.	21.3	100
33	Regional imaging genetic enrichment analysis. Bioinformatics, 2020, 36, 2554-2560.	4.1	16
34	Joint Multi-Modal Longitudinal Regression and Classification for Alzheimer's Disease Prediction. IEEE Transactions on Medical Imaging, 2020, 39, 1845-1855.	8.9	40
35	Multi-modal neuroimaging feature selection with consistent metric constraint for diagnosis of Alzheimer's disease. Medical Image Analysis, 2020, 60, 101625.	11.6	99
36	A multi-model deep convolutional neural network for automatic hippocampus segmentation and classification in Alzheimer's disease. NeuroImage, 2020, 208, 116459.	4.2	306

#	Article	IF	CITATIONS
37	Genetic correlations and genome-wide associations of cortical structure in general population samples of 22,824 adults. Nature Communications, 2020, 11, 4796.	12.8	61
38	Higher CSF sTREM2 attenuates ApoE4-related risk for cognitive decline and neurodegeneration. Molecular Neurodegeneration, 2020, 15, 57.	10.8	33
39	Volumetric GWAS of medial temporal lobe structures identifies an ERC1 locus using ADNI high-resolution T2-weighted MRI data. Neurobiology of Aging, 2020, 95, 81-93.	3.1	7
40	Identifying diagnosis-specific genotype–phenotype associations via joint multitask sparse canonical correlation analysis and classification. Bioinformatics, 2020, 36, i371-i379.	4.1	20
41	Analysis of the clinical characteristics of 176 patients with pathologically confirmed cryptogenic organizing pneumonia. Annals of Translational Medicine, 2020, 8, 763-763.	1.7	15
42	Cognitive biomarker prioritization in Alzheimer's Disease using brain morphometric data. BMC Medical Informatics and Decision Making, 2020, 20, 319.	3.0	4
43	A telescope GWAS analysis strategy, based on SNPs-genes-pathways ensamble and on multivariate algorithms, to characterize late onset Alzheimer's disease. Scientific Reports, 2020, 10, 12063.	3.3	11
44	Integrative analysis of summary data from GWAS and eQTL studies predicts tissueâ€specific gene targets for Alzheimer's disease. Alzheimer's and Dementia, 2020, 16, e043242.	0.8	2
45	Transcriptomic profiles underlying functional brain networks at different stages of Alzheimer's disease. Alzheimer's and Dementia, 2020, 16, e046163.	0.8	2
46	Genomeâ€wide association study of ADNI QTâ€₽AD biomarkers identifies a novel locus on Chr 12. Alzheimer's and Dementia, 2020, 16, e047579.	0.8	0
47	Ideas for how informaticians can get involved with COVID-19 research. BioData Mining, 2020, 13, 3.	4.0	20
48	Deep Network-Based Feature Selection for Imaging Genetics: Application to Identifying Biomarkers for Parkinson's Disease. , 2020, 2020, .		1
49	The use of ECMO in acute respiratory failure caused by <i>Pneumocystis jirovecii</i> pneumonia after renal transplant: A case report. Artificial Organs, 2020, 44, 1115-1117.	1.9	1
50	Mining and visualizing high-order directional drug interaction effects using the FAERS database. BMC Medical Informatics and Decision Making, 2020, 20, 50.	3.0	11
51	The genetic architecture of the human cerebral cortex. Science, 2020, 367, .	12.6	450
52	Pigmented purpuric dermatosis in children: a retrospective cohort with emphasis on treatment and outcomes. Journal of the European Academy of Dermatology and Venereology, 2020, 34, 2402-2408.	2.4	3
53	A superâ€comboâ€drug test to detect adverse drug events and drug interactions from electronic health records in the era of polypharmacy. Statistics in Medicine, 2020, 39, 1458-1472.	1.6	1
54	Detecting genetic associations with brain imaging phenotypes in Alzheimer's disease via a novel structured SCCA approach. Medical Image Analysis, 2020, 61, 101656.	11.6	53

#	Article	IF	CITATIONS
55	Therapeutic effect of subcutaneous injection of low dose recombinant human granulocyte-macrophage colony-stimulating factor on pulmonary alveolar proteinosis. Respiratory Research, 2020, 21, 1.	3.6	200
56	A report of three COVID-19 cases with prolonged viral RNA detection in anal swabs. Clinical Microbiology and Infection, 2020, 26, 786-787.	6.0	18
57	Associating Multi-Modal Brain Imaging Phenotypes and Genetic Risk Factors via a Dirty Multi-Task Learning Method. IEEE Transactions on Medical Imaging, 2020, 39, 3416-3428.	8.9	27
58	The International Conference on Intelligent Biology and Medicine (ICIBM) 2020: Data-driven analytics in biomedical genomics. BMC Medical Genomics, 2020, 13, 189.	1.5	2
59	Brain-wide structural connectivity alterations under the control of Alzheimer risk genes. International Journal of Computational Biology and Drug Design, 2020, 13, 58.	0.3	7
60	Genome-wide Network-assisted Association and Enrichment Study of Amyloid Imaging Phenotype in Alzheimer's Disease. Current Alzheimer Research, 2020, 16, 1163-1174.	1.4	11
61	Effect of APOE Îμ4 on multimodal brain connectomic traits: a persistent homology study. BMC Bioinformatics, 2020, 21, 535.	2.6	6
62	Informatics and machine learning methods for health applications. BMC Medical Informatics and Decision Making, 2020, 20, 342.	3.0	3
63	Multivariate genome wide association and network analysis of subcortical imaging phenotypes in Alzheimer's disease. BMC Genomics, 2020, 21, 896.	2.8	11
64	The International Conference on Intelligent Biology and Medicine (ICIBM) 2020: Scalable techniques and algorithms for computational genomics. BMC Genomics, 2020, 21, 831.	2.8	0
65	Accelerating bioinformatics research with International Conference on Intelligent Biology and Medicine 2020. BMC Bioinformatics, 2020, 21, 563.	2.6	2
66	Persistent Feature Analysis of Multimodal Brain Networks Using Generalized Fused Lasso for EMCI Identification. Lecture Notes in Computer Science, 2020, 12267, 44-52.	1.3	4
67	Structural Connectivity Enriched Functional Brain Network Using Simplex Regression with GraphNet. Lecture Notes in Computer Science, 2020, 12436, 292-302.	1.3	2
68	Predicting Longitudinal Outcomes of Alzheimer's Disease via a Tensor-Based Joint Classification and Regression Model. Pacific Symposium on Biocomputing Pacific Symposium on Biocomputing, 2020, 25, 7-18.	0.7	2
69	Deep Multiview Learning to Identify Population Structure with Multimodal Imaging. Proceedings IEEE International Symposium on Bioinformatics and Bioengineering, 2020, 2020, 308-314.	1.0	0
70	Polygenic mediation analysis of Alzheimer's disease implicated intermediate amyloid imaging phenotypes. AMIA Annual Symposium proceedings, 2020, 2020, 422-431.	0.2	0
71	Deep Multiview Learning to Identify Population Structure with Multimodal Imaging. , 2020, 2020, 308-314.		1
72	Estimating Hard-tissue Conditions from Dental Images via Machine Learning. , 2020, , .		0

Estimating Hard-tissue Conditions from Dental Images via Machine Learning. , 2020, , . 72

Li Shen

#	Article	IF	CITATIONS
73	Identifying Candidate Genetic Associations with MRI-Derived AD-Related ROI via Tree-Guided Sparse Learning. IEEE/ACM Transactions on Computational Biology and Bioinformatics, 2019, 16, 1986-1996.	3.0	8
74	Diagnosis Status Guided Brain Imaging Genetics Via Integrated Regression And Sparse Canonical Correlation Analysis. , 2019, 2019, 356-359.		9
75	Identifying progressive imaging genetic patterns via multi-task sparse canonical correlation analysis: a longitudinal study of the ADNI cohort. Bioinformatics, 2019, 35, i474-i483.	4.1	36
76	Targeted genetic analysis of cerebral blood flow imaging phenotypes implicates the INPP5D gene. Neurobiology of Aging, 2019, 81, 213-221.	3.1	30
77	Simultaneous amplification and testing method for <i>Mycobacterium tuberculosis</i> rRNA to differentiate sputum-negative tuberculosis from sarcoidosis. American Journal of Physiology - Lung Cellular and Molecular Physiology, 2019, 316, L519-L524.	2.9	11
78	Helicobacter pylori â€induced YAP1 nuclear translocation promotes gastric carcinogenesis by enhancing ILâ€1β expression. Cancer Medicine, 2019, 8, 3965-3980.	2.8	36
79	Identifying Imaging Markers for Predicting Cognitive Assessments Using Wasserstein Distances Based Matrix Regression. Frontiers in Neuroscience, 2019, 13, 668.	2.8	5
80	Lower dietary fibre intake, but not total water consumption, is associated with constipation: a populationâ€based analysis. Journal of Human Nutrition and Dietetics, 2019, 32, 422-431.	2.5	26
81	The Role of Infection in Acute Exacerbation of Idiopathic Pulmonary Fibrosis. Mediators of Inflammation, 2019, 2019, 1-10.	3.0	38
82	Preparing next-generation scientists for biomedical big data: artificial intelligence approaches. Personalized Medicine, 2019, 16, 247-257.	1.5	28
83	Prioritization of Cognitive Assessments in Alzheimer's Disease via Learning to Rank using Brain Morphometric Data. , 2019, 2019, .		2
84	Mining Regional Imaging Genetic Associations via Voxel-wise Enrichment Analysis. , 2019, 2019, .		4
85	Genetic architecture of subcortical brain structures in 38,851 individuals. Nature Genetics, 2019, 51, 1624-1636.	21.4	192
86	Joint between-sample normalization and differential expression detection through â,,"O-regularized regression. BMC Bioinformatics, 2019, 20, 593.	2.6	1
87	Mining Directional Drug Interaction Effects on Myopathy Using the FAERS Database. IEEE Journal of Biomedical and Health Informatics, 2019, 23, 2156-2163.	6.3	11
88	A Unified Model for Joint Normalization and Differential Gene Expression Detection in RNA-Seq Data. IEEE/ACM Transactions on Computational Biology and Bioinformatics, 2019, 16, 442-454.	3.0	13
89	A Dirty Multi-task Learning Method for Multi-modal Brain Imaging Genetics. Lecture Notes in Computer Science, 2019, , 447-455.	1.3	1
90	Improved Prediction of Cognitive Outcomes via Globally Aligned Imaging Biomarker Enrichments over Progressions. Lecture Notes in Computer Science, 2019, , 140-148.	1.3	4

#	Article	IF	CITATIONS
91	Predicting Longitudinal Outcomes of Alzheimer's Disease via a Tensor-Based Joint Classification and Regression Model. , 2019, , .		3
92	Network approaches to systems biology analysis of complex disease: integrative methods for multi-omics data. Briefings in Bioinformatics, 2018, 19, 1370-1381.	6.5	185
93	GPU Accelerated Browser for Neuroimaging Genomics. Neuroinformatics, 2018, 16, 393-402.	2.8	1
94	A novel SCCA approach via truncated <i> <b>â,,"</b> </i> 1-norm and truncated group lasso for brain imaging genetics. Bioinformatics, 2018, 34, 278-285.	4.1	31
95	Volumetric comparison of hippocampal subfields extracted from 4-minute accelerated vs. 8-minute high-resolution T2-weighted 3T MRI scans. Brain Imaging and Behavior, 2018, 12, 1583-1595.	2.1	13
96	Translational Highâ€Ðimensional Drug Interaction Discovery and Validation Using Health Record Databases and Pharmacokinetics Models. Clinical Pharmacology and Therapeutics, 2018, 103, 287-295.	4.7	22
97	Mixture drugâ€count response model for the highâ€dimensional drug combinatory effect on myopathy. Statistics in Medicine, 2018, 37, 673-686.	1.6	9
98	A Unified Model for Robust Differential Expression Analysis of RNA-Seq Data. , 2018, , .		0
99	Fast Multi-Task SCCA Learning with Feature Selection for Multi-Modal Brain Imaging Genetics. , 2018, 2018, 356-361.		13
100	Interactive Machine Learning by Visualization: A Small Data Solution. , 2018, 2018, 3513-3521.		16
101	ICâ€₽â€075: GENETIC FINDINGS USING ADNI MULTIMODAL QUANTITATIVE PHENOTYPES: A 2017 UPDATE. Alzheimer's and Dementia, 2018, 14, P66.	0.8	0
102	P2â€⊋35: GENETIC FINDINGS USING ADNI MULTIMODAL QUANTITATIVE PHENOTYPES: A 2018 UPDATE. Alzheimer's and Dementia, 2018, 14, P760.	0.8	0
103	Joint High-Order Multi-Task Feature Learning to Predict the Progression of Alzheimer's Disease. Lecture Notes in Computer Science, 2018, 11070, 555-562.	1.3	13
104	Quantitative trait loci identification for brain endophenotypes via new additive model with random networks. Bioinformatics, 2018, 34, i866-i874.	4.1	11
105	Predicting progressions of cognitive outcomes via high-order multi-modal multi-task feature learning. , 2018, , .		6
106	Multiple incomplete views clustering via non-negative matrix factorization with its application in Alzheimer's disease analysis. , 2018, , .		5
107	Bootstrapped Sparse Canonical Correlation Analysis. , 2018, , 101-117.		0
108	A Network-Based Framework for Mining High-Level Imaging Genetic Associations. , 2018, , 119-134.		0

#	Article	IF	CITATIONS
109	Longitudinal Genotype–Phenotype Association Study through Temporal Structure Auto-Learning Predictive Model. Journal of Computational Biology, 2018, 25, 809-824.	1.6	6
110	Pattern Discovery from High-Order Drug-Drug Interaction Relations. Journal of Healthcare Informatics Research, 2018, 2, 272-304.	7.6	2
111	Joint exploration and mining of memory-relevant brain anatomic and connectomic patterns via a three-way association model. , 2018, 2018, 6-9.		4
112	Heritability Estimation of Reliable Connectomic Features. Lecture Notes in Computer Science, 2018, 11083, 58-66.	1.3	8
113	Validation of EuroSCORE II in Chinese Patients Undergoing Coronary Artery Bypass Surgery. Heart Surgery Forum, 2018, 21, 036.	0.5	9
114	Endobronchial aspergilloma associated with idiopathic pulmonary fibrosis: a case report and review of the literature. Sarcoidosis Vasculitis and Diffuse Lung Diseases, 2018, 35, 95-96.	0.2	0
115	ENIGMA and the individual: Predicting factors that affect the brain in 35 countries worldwide. NeuroImage, 2017, 145, 389-408.	4.2	173
116	Serum Krebs von den Lungenâ€6 level as a diagnostic biomarker for interstitial lung disease in Chinese patients. Clinical Respiratory Journal, 2017, 11, 337-345.	1.6	40
117	Novel genetic loci associated with hippocampal volume. Nature Communications, 2017, 8, 13624.	12.8	250
118	Histone Chaperone ASF1A Predicts Poor Outcomes for Patients With Gastrointestinal Cancer and Drives Cancer Progression by Stimulating Transcription of β-Catenin Target Genes. EBioMedicine, 2017, 21, 104-116.	6.1	21
119	Network-based genome wide study of hippocampal imaging phenotype in Alzheimer's Disease to identify functional interaction modules. , 2017, 2017, 6170-6174.		1
120	Tissue-specific network-based genome wide study of amygdala imaging phenotypes to identify functional interaction modules. Bioinformatics, 2017, 33, 3250-3257.	4.1	23
121	Mining Outcome-relevant Brain Imaging Genetic Associations via Three-way Sparse Canonical Correlation Analysis in Alzheimer's Disease. Scientific Reports, 2017, 7, 44272.	3.3	44
122	High throughput 16SrRNA gene sequencing reveals the correlation between Propionibacterium acnes and sarcoidosis. Respiratory Research, 2017, 18, 28.	3.6	27
123	Metabolic network failures in Alzheimer's disease: A biochemical roadÂmap. Alzheimer's and Dementia, 2017, 13, 965-984.	0.8	362
124	Brain explorer for connectomic analysis. Brain Informatics, 2017, 4, 253-269.	3.0	4
125	Predicting High-Order Directional Drug-Drug Interaction Relations. , 2017, , .		3

#	Article	IF	CITATIONS
127	BECA: A Software Tool for Integrated Visualization of Human Brain Data. Lecture Notes in Computer Science, 2017, , 285-291.	1.3	0
128	Genome-wide association and interaction studies of CSF T-tau/Aβ42 ratio in ADNI cohort. Neurobiology of Aging, 2017, 57, 247.e1-247.e8.	3.1	34
129	Association analysis of rare variants near the APOE region with CSF and neuroimaging biomarkers of Alzheimer's disease. BMC Medical Genomics, 2017, 10, 29.	1.5	28
130	Genome-wide network-based pathway analysis of CSF t-tau/Aβ1-42 ratio in the ADNI cohort. BMC Genomics, 2017, 18, 421.	2.8	13
131	Two-dimensional enrichment analysis for mining high-level imaging genetic associations. Brain Informatics, 2017, 4, 27-37.	3.0	13
132	Pattern Discovery in Brain Imaging Genetics via SCCA Modeling with a Generic Non-convex Penalty. Scientific Reports, 2017, 7, 14052.	3.3	9
133	Pattern Discovery from Directional High-Order Drug-Drug Interaction Relations. , 2017, , .		4
134	[P2–220]: GENETIC FINDINGS USING ADNI MULTIMODAL QUANTITATIVE PHENOTYPES: A 2016 UPDATE. Alzheimer's and Dementia, 2017, 13, P694.	0.8	0
135	[F1–02–04]: INTEGRATING MULTIâ€MODALITY IMAGING AND MULTIâ€LAYER â€OMICS TO ADVANCE THE S BIOLOGY OF ALZHEIMER's DISEASE. Alzheimer's and Dementia, 2017, 13, P175.	YSTEMS	0
136	IDENTIFICATION OF DISCRIMINATIVE IMAGING PROTEOMICS ASSOCIATIONS IN ALZHEIMER'S DISEASE VIA A NOVEL SPARSE CORRELATION MODEL. , 2017, 22, 94-104.		14
137	0049 SLEEP AND RELATIONSHIP DURING PREGNANCY: ASSOCIATIONS AND MECHANISMS. Sleep, 2017, 40, A19-A19.	1.1	0
138	Identification of associations between genotypes and longitudinal phenotypes via temporally-constrained group sparse canonical correlation analysis. Bioinformatics, 2017, 33, i341-i349.	4.1	42
139	Statistical Shape Analysis for Brain Structures. , 2017, , 351-378.		4
140	Stimulator of Interferon Genes Deficiency in Acute Exacerbation of Idiopathic Pulmonary Fibrosis. Frontiers in Immunology, 2017, 8, 1756.	4.8	27
141	Mapping longitudinal scientific progress, collaboration and impact of the Alzheimer's disease neuroimaging initiative. PLoS ONE, 2017, 12, e0186095.	2.5	10
142	Parcellation of Human Amygdala Subfields Using Orientation Distribution Function and Spectral K-means Clustering. Mathematics and Visualization, 2017, 2016, 123-132.	0.6	1
143	Longitudinal Genotype-Phenotype Association Study via Temporal Structure Auto-learning Predictive Model. Lecture Notes in Computer Science, 2017, 10229, 287-302.	1.3	8
144	Predicting Interrelated Alzheimer's Disease Outcomes via New Self-learned Structured Low-Rank Model. Lecture Notes in Computer Science, 2017, 10265, 198-209.	1.3	4

#	Article	IF	CITATIONS
145	Identifying Associations Between Brain Imaging Phenotypes and Genetic Factors via a Novel Structured SCCA Approach. Lecture Notes in Computer Science, 2017, 10265, 543-555.	1.3	12
146	Machine Learning for Large-Scale Quality Control of 3D Shape Models in Neuroimaging. Lecture Notes in Computer Science, 2017, 10541, 371-378.	1.3	4
147	Transcriptome-Guided Imaging Genetic Analysis via a Novel Sparse CCA Algorithm. Lecture Notes in Computer Science, 2017, 10551, 220-229.	1.3	5
148	Machine learning in brain imaging genomics. , 2016, , 411-434.		2
149	Exosomes from Human Umbilical Cord Mesenchymal Stem Cells: Identification, Purification, and Biological Characteristics. Stem Cells International, 2016, 2016, 1-11.	2.5	80
150	Building a surface atlas of hippocampal subfields from high resolution T2-weighted MRI scans using landmark-free surface registration. , 2016, 2016, .		1
151	Sparse Canonical Correlation Analysis via truncated â,," <inf>1</inf> -norm with application to brain imaging genetics. , 2016, 2016, 707-711.		6
152	New Probabilistic Multi-graph Decomposition Model to Identify Consistent Human Brain Network Modules. , 2016, 2016, 301-310.		1
153	O1â€12â€02: Identification of Discriminative Brain Imaging and Genomic Associations: an Alzheimer's Disease Study. Alzheimer's and Dementia, 2016, 12, P205.	0.8	0
154	ICâ€Pâ€075: The Growth and Impact of ADNI Genetics Publications as Measured by Science Mapping. Alzheimer's and Dementia, 2016, 12, P60.	0.8	0
155	P2â€098: Whole Brain Surfaceâ€Based Analysis Identified Brain Atrophy Associated with SNPS in <i>FRMD6</i> Linked to Alzheimer's Disease. Alzheimer's and Dementia, 2016, 12, P648.	0.8	2
156	P2â€258: The Growth and Impact of ADNI Genetics Publications as Measured by Science Mapping. Alzheimer's and Dementia, 2016, 12, P725.	0.8	0
157	P3-089: Influence of Parkinson's Disease Candidate Genes On Lewy Body Pathology in Autopsy-Confirmed Alzheimer's Disease Cases. , 2016, 12, P854-P854.		0
158	F1-02-02: Genetic Influence on Levels of Targeted Metabolites Associated with Alzheimer's Disease. , 2016, 12, P164-P165.		0
159	P4-344: Volumetric Comparison of Automatically Segmented Hippocampal Subfields From 4-Min Accelerated Versus 8-Min T2-Weighted 3T Mri Scans. , 2016, 12, P1167-P1167.		0
160	Identifying significant geneâ€environment interactions using a combination of screening testing and hierarchical false discovery rate control. Genetic Epidemiology, 2016, 40, 544-557.	1.3	20
161	Novel genetic loci underlying human intracranial volume identified through genome-wide association. Nature Neuroscience, 2016, 19, 1569-1582.	14.8	213
162	Transcription factor c-jun regulates β3Gn-T8 expression in gastric cancer cell line SGC-7901. Oncology Reports, 2016, 36, 1353-1360.	2.6	6

#	Article	IF	CITATIONS
163	A New Statistical Image Analysis Approach and Its Application to Hippocampal Morphometry. Lecture Notes in Computer Science, 2016, 9805, 302-310.	1.3	1
164	DIAGNOSIS-GUIDED METHOD FOR IDENTIFYING MULTI-MODALITY NEUROIMAGING BIOMARKERS ASSOCIATED WITH GENETIC RISK FACTORS IN ALZHEIMER'S DISEASE. , 2016, , .		4
165	Structured sparse CCA for brain imaging genetics via graph OSCAR. BMC Systems Biology, 2016, 10, 68.	3.0	9
166	Identifying Multimodal Intermediate Phenotypes Between Genetic Risk Factors and Disease Status in Alzheimer's Disease. Neuroinformatics, 2016, 14, 439-452.	2.8	26
167	Network-based analysis of genetic variants associated with hippocampal volume in Alzheimer's disease: a study of ADNI cohorts. BioData Mining, 2016, 9, 3.	4.0	28
168	Structured sparse canonical correlation analysis for brain imaging genetics: an improved GraphNet method. Bioinformatics, 2016, 32, 1544-1551.	4.1	96
169	Clinical Characteristics of Connective Tissue Disease-Associated Interstitial Lung Disease in 1,044 Chinese Patients. Chest, 2016, 149, 201-208.	0.8	58
170	Mutual amplification of HNF4α and IL-1R1 composes an inflammatory circuit in <i>Helicobacter pylori</i> associated gastric carcinogenesis. Oncotarget, 2016, 7, 11349-11363.	1.8	12
171	DIAGNOSIS-GUIDED METHOD FOR IDENTIFYING MULTI-MODALITY NEUROIMAGING BIOMARKERS ASSOCIATED WITH GENETIC RISK FACTORS IN ALZHEIMER'S DISEASE. Pacific Symposium on Biocomputing Pacific Symposium on Biocomputing, 2016, 21, 108-19.	0.7	3
172	P3-134: Association of eye disease with increased diffusivity in the sagittal stratum. , 2015, 11, P675-P675.		0
173	P1-201: Genetic findings using ADNI multimodal quantitative phenotypes: A 2014 update. , 2015, 11, P426-P426.		1
174	P1-193: Anticholinergic medication use in older adults is associated with memory and hippocampal volume. , 2015, 11, P422-P422.		0
175	IC-P-035: Effect of hypertension and antihypertensive medication on executive function, brain atrophy, and white matter hyperintensities. , 2015, 11, P32-P33.		0
176	P4-002: Genome-wide network-based pathway analysis of CSF biomarker t-tau in the ADNI cohort. , 2015, 11, P765-P765.		0
177	P4-008: Mapre2 as a novel Alzheimer's disease target gene from gwas of CSF amyloid beta 1-42, tau and hyperphosphorylated tau in the ADNI cohort. , 2015, 11, P767-P768.		3
178	IC-P-034: Anticholinergic medication use in older adults is associated with memory and hippocampal volume. , 2015, 11, P32-P32.		0
179	Graphic Mining of Highâ€Order Drug Interactions and Their Directional Effects on Myopathy Using Electronic Medical Records. CPT: Pharmacometrics and Systems Pharmacology, 2015, 4, 481-488.	2.5	15
180	IC-P-036: Association of eye disease with increased diffusivity in the sagittal stratum. , 2015, 11, P33-P33.		0

#	Article	IF	CITATIONS
181	O4-05-01: Gwas of longitudinal amyloid PET identifies IL1RAP as a new potential Alzheimer's disease target. , 2015, 11, P277-P278.		0
182	The role of visualization and 3-D printing in biological data mining. BioData Mining, 2015, 8, 22.	4.0	5
183	Frequency-specific adaptation and its underlying circuit model in the auditory midbrain. Frontiers in Neural Circuits, 2015, 9, 55.	2.8	15
184	Genetic Interactions Explain Variance in Cingulate Amyloid Burden: An AV-45 PET Genome-Wide Association and Interaction Study in the ADNI Cohort. BioMed Research International, 2015, 2015, 1-11.	1.9	24
185	A Mixture Dose–Response Model for Identifying Highâ€Dimensional Drug Interaction Effects on Myopathy Using Electronic Medical Record Databases. CPT: Pharmacometrics and Systems Pharmacology, 2015, 4, 474-480.	2.5	12
186	O1-04-04: Effect of hypertension and antihypertensive medication on executive function, brain atrophy, and white matter hyperintensities. , 2015, 11, P133-P134.		0
187	P1-009: The nav2 (neuron navigator 2) gene as a common genetic influence across correlated episodic memory performances. , 2015, 11, P339-P340.		0
188	O3-13-04: Genome-wide rare variant analysis identifies candidate genes significantly associated with composite scores for memory. , 2015, 11, P251-P252.		1
189	O4-12-06: The Alzheimer's metabolome: Identification of novel markers and treatment targets. , 2015, 11, P301-P302.		0
190	Cortical surface biomarkers for predicting cognitive outcomes using group l2,1 norm. Neurobiology of Aging, 2015, 36, S185-S193.	3.1	43
191	Protective variant for hippocampal atrophy identified by whole exome sequencing. Annals of Neurology, 2015, 77, 547-552.	5.3	48
192	Common genetic variants influence human subcortical brain structures. Nature, 2015, 520, 224-229.	27.8	772
193	2014 Update of the Alzheimer's Disease Neuroimaging Initiative: AÂreview of papers published since its inception. Alzheimer's and Dementia, 2015, 11, e1-120.	0.8	261
194	Treatment of cholestatic fibrosis by altering gene expression of Cthrc1: Implications for autoimmune and non-autoimmune liver disease. Journal of Autoimmunity, 2015, 63, 76-87.	6.5	30
195	Genetic studies of quantitative MCI and AD phenotypes in ADNI: Progress, opportunities, and plans. Alzheimer's and Dementia, 2015, 11, 792-814.	0.8	241
196	Hippocampal transcriptome-guided genetic analysis of correlated episodic memory phenotypes in Alzheimer's disease. Frontiers in Genetics, 2015, 6, 117.	2.3	23
197	<i>APOE</i> effect on Alzheimer's disease biomarkers in older adults with significant memory concern. Alzheimer's and Dementia, 2015, 11, 1417-1429.	0.8	157
198	Surface-based morphometric analysis of hippocampal subfields in mild cognitive impairment and Alzheimer's disease. , 2015, 2015, .		5

#	Article	IF	CITATIONS
199	Two-Dimensional Enrichment Analysis for Mining High-Level Imaging Genetic Associations. Lecture Notes in Computer Science, 2015, 9250, 115-124.	1.3	1
200	GWAS of longitudinal amyloid accumulation on <sup>18</sup> F-florbetapir PET in Alzheimer's disease implicates microglial activation gene <i>IL1RAP</i> . Brain, 2015, 138, 3076-3088.	7.6	117
201	Computed tomography assessment of peripubertal craniofacial morphology in a sheep model of binge alcohol drinking in the first trimester. Alcohol, 2015, 49, 675-689.	1.7	5
202	FASTKD2 is associated with memory and hippocampal structure in older adults. Molecular Psychiatry, 2015, 20, 1197-1204.	7.9	33
203	GN-SCCA: GraphNet Based Sparse Canonical Correlation Analysis for Brain Imaging Genetics. Lecture Notes in Computer Science, 2015, 9250, 275-284.	1.3	14
204	Integrated Visualization of Human Brain Connectome Data. Lecture Notes in Computer Science, 2015, 9250, 295-305.	1.3	4
205	Identifying Connectome Module Patterns via New Balanced Multi-graph Normalized Cut. Lecture Notes in Computer Science, 2015, 9350, 169-176.	1.3	4
206	Histone demethylase RBP2 promotes malignant progression of gastric cancer through TGF-β1-(p-Smad3)-RBP2-E-cadherin-Smad3 feedback circuit. Oncotarget, 2015, 6, 17661-17674.	1.8	30
207	Accelerating Sparse Canonical Correlation Analysis for Large Brain Imaging Genetics Data. , 2014, , .		0
208	Joint identification of imaging and proteomics biomarkers of Alzheimer's disease using network-guided sparse learning. , 2014, 2014, 665-668.		1
209	Data synthesis and method evaluation for brain imaging genetics. , 2014, 2014, 1202-1205.		6
210	β3GnT8 regulates the metastatic potential of colorectal carcinoma cells by altering the glycosylation of CD147. Oncology Reports, 2014, 31, 1795-1801.	2.6	23
211	P3-018: INFLUENCE OF RARE PSEN1 VARIANTS ON QUANTITATIVE STRUCTURAL IMAGING AND CSF PHENOTYPES IN LATE ONSET ALZHEIMER'S DISEASE. , 2014, 10, P633-P633.		0
212	Building a surface atlas of hippocampal subfields from MRI scans using FreeSurfer, FIRST and SPHARM. , 2014, 2014, 813-816.		10
213	Transcriptome-guided amyloid imaging genetic analysis via a novel structured sparse learning algorithm. Bioinformatics, 2014, 30, i564-i571.	4.1	57
214	Genetic analysis of quantitative phenotypes in AD and MCI: imaging, cognition and biomarkers. Brain Imaging and Behavior, 2014, 8, 183-207.	2.1	161
215	The ENIGMA Consortium: large-scale collaborative analyses of neuroimaging and genetic data. Brain Imaging and Behavior, 2014, 8, 153-182.	2.1	696
216	Computational genetics analysis of grey matter density in Alzheimer's disease. BioData Mining, 2014, 7, 17.	4.0	6

#	Article	IF	CITATIONS
217	Identifying the Neuroanatomical Basis of Cognitive Impairment in Alzheimer's Disease by Correlation- and Nonlinearity-Aware Sparse Bayesian Learning. IEEE Transactions on Medical Imaging, 2014, 33, 1475-1487.	8.9	49
218	Association of plasma and cortical amyloid beta is modulated by <i>APOE</i> ε4 status. Alzheimer's and Dementia, 2014, 10, e9-e18.	0.8	43
219	APOE and BCHE as modulators of cerebral amyloid deposition: a florbetapir PET genome-wide association study. Molecular Psychiatry, 2014, 19, 351-357.	7.9	181
220	IC-P-172: GENOME-WIDE PROTEIN INTERACTION GUIDED EPISTATIC ANALYSIS ON MEMORY PERFORMANCE: AN ADNI STUDY. , 2014, 10, P95-P96.		0
221	Improving protein order-disorder classification using charge-hydropathy plots. BMC Bioinformatics, 2014, 15, S4.	2.6	63
222	IC-P-173: EFFECTS OF NEWLY IDENTIFIED TOP AD CANDIDATE GENES ON MEMORY PERFORMANCE: SNP, GENE, AND EPISTASIS ANALYSES IN ADNI. , 2014, 10, P96-P97.		0
223	IC-P-177: GENETIC FINDINGS USING ADNI MULTIMODAL QUANTITATIVE PHENOTYPES: A REVIEW OF PAPERS PUBLISHED IN 2013. , 2014, 10, P99-P100.		0
224	P1-230: EFFECTS OF NEWLY IDENTIFIED TOP AD CANDIDATE GENES ON MEMORY PERFORMANCE: SNP, GENE, AND EPISTASIS ANALYSES IN ADNI. , 2014, 10, P388-P388.		0
225	IC-P-174: RARE VARIANT IN PLD3 IS ASSOCIATED WITH ALZHEIMER'S PATTERN OF NEURODEGENERATIVE CHANGES. , 2014, 10, P97-P97.		0
226	P3-024: NEXT-GENERATION SEQUENCING OF THE BCHE LOCUS IDENTIFIES A FUNCTIONAL SNP ASSOCIATED WITH ALZHEIMER'S DISEASE BIOMARKERS AND AGE OF ONSET. , 2014, 10, P636-P636.		0
227	P4-054: ASSOCIATION OF PLASMA LEPTIN/ADIPONECTIN RATIO IN MEN WITH CSF BIOMARKERS IN THE ADNI-1 COHORT. , 2014, 10, P801-P802.		0
228	P1-213: GENOME-WIDE PROTEIN INTERACTION-GUIDED EPISTATIC ANALYSIS ON MEMORY PERFORMANCE: AN ADNI STUDY. , 2014, 10, P381-P382.		0
229	P3-017: ASSOCIATION ANALYSIS OF RARE VARIANTS NEAR THE APOE REGION WITH CEREBROSPINAL FLUID (CSF) BIOMARKERS OF ALZHEIMER'S DISEASE. , 2014, 10, P632-P633.		0
230	P1-141: GENETIC FINDINGS USING ADNI MULTIMODAL QUANTITATIVE PHENOTYPES: A REVIEW OF PAPERS PUBLISHED IN 2013. , 2014, 10, P351-P351.		0
231	P3-019: RARE VARIANT IN PLD3 IS ASSOCIATED WITH ALZHEIMER'S PATTERN OF NEURODEGENERATIVE CHANGES. , 2014, 10, P634-P634.		0
232	P4-237: WHOLE GENE-BASED ASSOCIATION OF BASELINE PLASMA HOMOCYSTEINE IN THE ADNI-1 COHORT. , 2014, 10, P873-P874.		0
233	Human Connectome Module Pattern Detection Using a New Multi-graph MinMax Cut Model. Lecture Notes in Computer Science, 2014, 17, 313-320.	1.3	9
234	A Novel Structure-Aware Sparse Learning Algorithm for Brain Imaging Genetics. Lecture Notes in Computer Science, 2014, 17, 329-336.	1.3	36

#	Article	IF	CITATIONS
235	Histone demethylase RBP2 induced by Helicobactor Pylori CagA participates in the malignant transformation of gastric epithelial cells. Oncotarget, 2014, 5, 5798-5807.	1.8	16
236	Interactive object extraction by merging regions with k-global maximal similarity. Neurocomputing, 2013, 120, 610-623.	5.9	5
237	IC-O1-03: Hippocampal transcriptome-guided gene-gene interaction of memory phenotype in MCI and Alzheimer's disease. , 2013, 9, P4-P4.		0
238	Meta-Analysis of Cohort Studies of Baseline Prehypertension and Risk of Coronary Heart Disease. American Journal of Cardiology, 2013, 112, 266-271.	1.6	77
239	Genome-wide scan of healthy human connectome discovers <i>SPON1</i> gene variant influencing dementia severity. Proceedings of the National Academy of Sciences of the United States of America, 2013, 110, 4768-4773.	7.1	141
240	Effect of prenatal alcohol exposure on bony craniofacial development: A mouse MicroCT study. Alcohol, 2013, 47, 405-415.	1.7	23
241	The Alzheimer's Disease Neuroimaging Initiative: A review of papers published since its inception. Alzheimer's and Dementia, 2013, 9, e111-94.	0.8	535
242	Whole-exome sequencing and imaging genetics identify functional variants for rate of change in hippocampal volume in mild cognitive impairment. Molecular Psychiatry, 2013, 18, 781-787.	7.9	81
243	Identification of functional variants from whole-exome sequencing, combined with neuroimaging genetics. Molecular Psychiatry, 2013, 18, 739-739.	7.9	8
244	Development of Refractive Error in Individual Children With Regressed Retinopathy of Prematurity. , 2013, 54, 6018.		58
245	Influence of <i>TSPO</i> Genotype on <sup>11</sup> C-PBR28 Standardized Uptake Values. Journal of Nuclear Medicine, 2013, 54, 1320-1322.	5.0	56
246	The role of apolipoprotein E (APOE) genotype in early mild cognitive impairment (E-MCI). Frontiers in Aging Neuroscience, 2013, 5, 11.	3.4	126
247	PARP1 Gene Variation and Microglial Activity on [11C]PBR28 PET in Older Adults at Risk for Alzheimer's Disease. Lecture Notes in Computer Science, 2013, 8159, 150-158.	1.3	8
248	A Graph-Based Integration of Multimodal Brain Imaging Data for the Detection of Early Mild Cognitive Impairment (E-MCI). Lecture Notes in Computer Science, 2013, 8159, 159-169.	1.3	10
249	Network-Guided Sparse Learning for Predicting Cognitive Outcomes from MRI Measures. Lecture Notes in Computer Science, 2013, 8159, 202-210.	1.3	5
250	A New Sparse Simplex Model for Brain Anatomical and Genetic Network Analysis. Lecture Notes in Computer Science, 2013, 16, 625-632.	1.3	12
251	Influence of Genetic Variation on Plasma Protein Levels in Older Adults Using a Multi-Analyte Panel. PLoS ONE, 2013, 8, e70269.	2.5	50
252	Genetic Clustering on the Hippocampal Surface for Genome-Wide Association Studies. Lecture Notes in Computer Science, 2013, 16, 690-697.	1.3	7

#	Article	IF	CITATIONS
253	Structural Brain Network Constrained Neuroimaging Marker Identification for Predicting Cognitive Functions. Lecture Notes in Computer Science, 2013, 23, 536-547.	1.3	3
254	Identifying disease sensitive and quantitative trait-relevant biomarkers from multidimensional heterogeneous imaging genetics data via sparse multimodal multitask learning. Bioinformatics, 2012, 28, i127-i136.	4.1	114
255	Analysis of Copy Number Variation in Alzheimer's Disease: The NIALOAD/ NCRAD Family Study. Current Alzheimer Research, 2012, 9, 801-814.	1.4	64
256	Association of common genetic variants in GPCPD1 with scaling of visual cortical surface area in humans. Proceedings of the National Academy of Sciences of the United States of America, 2012, 109, 3985-3990.	7.1	50
257	Multimodal Neuroimaging Predictors for Cognitive Performance Using Structured Sparse Learning. Lecture Notes in Computer Science, 2012, , 1-17.	1.3	4
258	From phenotype to genotype: an association study of longitudinal phenotypic markers to Alzheimer's disease relevant SNPs. Bioinformatics, 2012, 28, i619-i625.	4.1	62
259	Identifying quantitative trait loci via group-sparse multitask regression and feature selection: an imaging genetics study of the ADNI cohort. Bioinformatics, 2012, 28, 229-237.	4.1	149
260	O4â€01â€01: Classification of MCI and Alzheimer's disease from CSF biomarkers: An ADNI study of Aß, tau and Pâ€ŧau versus 83 proteomic analytes. Alzheimer's and Dementia, 2012, 8, P609.	0.8	0
261	Sparse Bayesian multi-task learning for predicting cognitive outcomes from neuroimaging measures in Alzheimer's disease. , 2012, , .		15
262	Identification of common variants associated with human hippocampal and intracranial volumes. Nature Genetics, 2012, 44, 552-561.	21.4	594
263	Tea consumption and risk of stroke: a dose-response meta-analysis of prospective studies. Journal of Zhejiang University: Science B, 2012, 13, 652-662.	2.8	42
264	A large scale multivariate parallel ICA method reveals novel imaging–genetic relationships for Alzheimer's disease in the ADNI cohort. NeuroImage, 2012, 60, 1608-1621.	4.2	111
265	Cenome-wide pathway analysis of memory impairment in the Alzheimer's Disease Neuroimaging Initiative (ADNI) cohort implicates gene candidates, canonical pathways, and networks. Brain Imaging and Behavior, 2012, 6, 634-648.	2.1	58
266	Voxel and surface-based topography of memory and executive deficits in mild cognitive impairment and Alzheimer's disease. Brain Imaging and Behavior, 2012, 6, 551-567.	2.1	66
267	Analysis of Copy Number Variation in Alzheimer's Disease in a Cohort of Clinically Characterized and Neuropathologically Verified Individuals. PLoS ONE, 2012, 7, e50640.	2.5	49
268	Multiple loci influencing hippocampal degeneration identified by genome scan. Annals of Neurology, 2012, 72, 65-75.	5.3	59
269	Pathway analysis of genomic data: concepts, methods, and prospects for future development. Trends in Genetics, 2012, 28, 323-332.	6.7	237
270	Amyloid pathway-based candidate gene analysis of [11C]PiB-PET in the Alzheimer's Disease Neuroimaging Initiative (ADNI) cohort. Brain Imaging and Behavior, 2012, 6, 1-15.	2.1	47

#	Article	IF	CITATIONS
271	The Interleukin 3 Gene (IL3) Contributes to Human Brain Volume Variation by Regulating Proliferation and Survival of Neural Progenitors. PLoS ONE, 2012, 7, e50375.	2.5	33
272	The Stereology and 3D Volume Analyses in Nervous Tissue. Springer Protocols, 2012, , 31-52.	0.3	0
273	Voxelwise gene-wide association study (vGeneWAS): Multivariate gene-based association testing in 731 elderly subjects. NeuroImage, 2011, 56, 1875-1891.	4.2	116
274	Regional reproducibility of pulsed arterial spin labeling perfusion imaging at 3T. NeuroImage, 2011, 54, 1188-1195.	4.2	79
275	Sparse multi-task regression and feature selection to identify brain imaging predictors for memory performance. , 2011, , 557-562.		72
276	Genomic Copy Number Analysis in Alzheimer's Disease and Mild Cognitive Impairment: An ADNI Study. International Journal of Alzheimer's Disease, 2011, 2011, 1-10.	2.0	51
277	FOURIER METHODS FOR 3D SURFACE MODELING AND ANALYSIS. Series in Computer Vision, 2011, , 175-196.	0.1	2
278	Genome-wide association with MRI atrophy measures as a quantitative trait locus for Alzheimer's disease. Molecular Psychiatry, 2011, 16, 1130-1138.	7.9	133
279	Genome-wide association study of CSF biomarkers Aβ <sub>1-42</sub> , t-tau, and p-tau <sub>181p</sub> in the ADNI cohort. Neurology, 2011, 76, 69-79.	1.1	185
280	Identifying AD-Sensitive and Cognition-Relevant Imaging Biomarkers via Joint Classification and Regression. Lecture Notes in Computer Science, 2011, 14, 115-123.	1.3	57
281	Hippocampal Surface Mapping of Genetic Risk Factors in AD via Sparse Learning Models. Lecture Notes in Computer Science, 2011, 14, 376-383.	1.3	20
282	Identifying Neuroimaging and Proteomic Biomarkers for MCI and AD via the Elastic Net. Lecture Notes in Computer Science, 2011, 7012, 27-34.	1.3	53
283	The effect of reference panels and software tools on genotype imputation. AMIA Annual Symposium proceedings, 2011, 2011, 1013-8.	0.2	8
284	Comparison of Manual and Automated Determination of Hippocampal Volumes in MCI and Early AD. Brain Imaging and Behavior, 2010, 4, 86-95.	2.1	74
285	Genetic pathwayâ€based hierarchical clustering analysis of older adults with cognitive complaints and amnestic mild cognitive impairment using clinical and neuroimaging phenotypes. American Journal of Medical Genetics Part B: Neuropsychiatric Genetics, 2010, 153B, 1060-1069.	1.7	31
286	A commonly carried allele of the obesity-related <i>FTO</i> gene is associated with reduced brain volume in the healthy elderly. Proceedings of the National Academy of Sciences of the United States of America, 2010, 107, 8404-8409.	7.1	227
287	Voxelwise genome-wide association study (vGWAS). NeuroImage, 2010, 53, 1160-1174.	4.2	239
288	Genome-wide analysis reveals novel genes influencing temporal lobe structure with relevance to neurodegeneration in Alzheimer's disease. NeuroImage, 2010, 51, 542-554.	4.2	141

#	Article	IF	CITATIONS
289	Longitudinal MRI atrophy biomarkers: Relationship to conversion in the ADNI cohort. Neurobiology of Aging, 2010, 31, 1401-1418.	3.1	230
290	Alzheimer's Disease Neuroimaging Initiative biomarkers as quantitative phenotypes: Genetics core aims, progress, and plans. Alzheimer's and Dementia, 2010, 6, 265-273.	0.8	378
291	IC-01-04: Neuroinflammation and amyloid deposition: Concurrent [11 C]PBR28 and [11 C]PIB PET imaging in patients with Alzheimer's disease, mild cognitive impairment, and older adults with cognitive complaints. , 2010, 6, S3-S4.		3
292	O3-O3-O1: Genome-wide association study of CSF biomarkers amyloid beta 1-42, tau and tau phosphorylated at threonine 181 in the ADNI cohort. , 2010, 6, S129-S129.		1
293	O3-06-01: Association analysis of candidate SNPs on hippocampal volume and shape in mild cognitive impairment and older adults with cognitive complaints. , 2010, 6, S137-S138.		1
294	Whole genome association study of brain-wide imaging phenotypes for identifying quantitative trait loci in MCI and AD: A study of the ADNI cohort. NeuroImage, 2010, 53, 1051-1063.	4.2	340
295	Apolipoprotein E (APOE) genotype has dissociable effects on memory and attentional–executive network function in Alzheimer's disease. Proceedings of the National Academy of Sciences of the United States of America, 2010, 107, 10256-10261.	7.1	215
296	Sparse Bayesian Learning for Identifying Imaging Biomarkers in AD Prediction. Lecture Notes in Computer Science, 2010, 13, 611-618.	1.3	21
297	Automatic Prediction of Conversion from Mild Cognitive Impairment to Probable Alzheimer's Disease using Structural Magnetic Resonance Imaging. AMIA Annual Symposium proceedings, 2010, 2010, 542-6.	0.2	8
298	Visual exploration of genetic association with voxel-based imaging phenotypes in an MCI/AD study. , 2009, 2009, 3849-52.		2
299	Baseline MRI Predictors of Conversion from MCI to Probable AD in the ADNI Cohort. Current Alzheimer Research, 2009, 6, 347-361.	1.4	484
300	Fourier method for large-scale surface modeling and registration. Computers and Graphics, 2009, 33, 299-311.	2.5	23
301	Parametric surface modeling and registration for comparison of manual and automated segmentation of the hippocampus. Hippocampus, 2009, 19, 588-595.	1.9	32
302	THE CORRELATED EVOLUTION OF THREE-DIMENSIONAL REPRODUCTIVE STRUCTURES BETWEEN MALE AND FEMALE DAMSELFLIES. Evolution; International Journal of Organic Evolution, 2009, 63, 73-83.	2.3	94
303	MODELING THREE-DIMENSIONAL MORPHOLOGICAL STRUCTURES USING SPHERICAL HARMONICS. Evolution; International Journal of Organic Evolution, 2009, 63, 1003-1016.	2.3	195
304	Data synthesis and tool development for exploring imaging genomic patterns. , 2009, 2009, 298-305.		3
305	Mining 3D Shape Data for Morphometric Pattern Discovery. , 2009, , 1236-1242.		0
306	The Tempo and Mode of Threeâ€Dimensional Morphological Evolution in Male Reproductive Structures. American Naturalist, 2008, 171, E158-E178.	2.1	140

#	Article	IF	CITATIONS
307	Computational Issues in Biomedical Nanometrics and Nano-Materials. Journal of Nano Research, 2008, 1, 50-58.	0.8	3
308	Weighted Fourier Series Representation and Its Application to Quantifying the Amount of Gray Matter. IEEE Transactions on Medical Imaging, 2007, 26, 566-581.	8.9	161
309	Surface Harmonics for Shape Modeling. , 2007, , .		0
310	Morphometric Analysis of Hippocampal Shape in Mild Cognitive Impairment: An Imaging Genetics Study. , 2007, , .		9
311	Efficient Registration of 3D SPHARM Surfaces. , 2007, , .		20
312	Hippocampal Volume and Shape Analysis in an Older Adult Population. Clinical Neuropsychologist, 2007, 21, 130-145.	2.3	28
313	Three-dimensional Models for Cardiac Bioelectricity Simulation: Cell to Organ. Simulation, 2007, 83, 321-327.	1.8	2
314	Inhibition of human neutrophil degranulation by transforming growth factor-β1. Clinical and Experimental Immunology, 2007, 149, 155-161.	2.6	57
315	A Novel Surface Registration Algorithm With Biomedical Modeling Applications. IEEE Transactions on Information Technology in Biomedicine, 2007, 11, 474-482.	3.2	19
316	Cardiac Motion Analysis to Improve Pacing Site Selection in CRT. Academic Radiology, 2006, 13, 1124-1134.	2.5	14
317	Spatio-temporal modeling of lung images for cancer detection. Oncology Reports, 2006, 15 Spec no., 1085-9.	2.6	2
318	Measuring blood delivery to solitary pulmonary nodules using perfusion magnetic resonance imaging. , 2006, , .		0
319	Spatio-temporal analysis tool for modeling pulmonary nodules in MR images. , 2006, 6141, 740.		1
320	Fast surface alignment for cardiac spatio-temporal modeling: application to Ischemic cardiac shape modeling. , 2006, , .		0
321	Hemispherical Harmonic Surface Description and Applications to Medical Image Analysis. , 2006, , .		4
322	Shape Analysis and Spatio-Temporal Tracking of Mesoscale Eddies in Miami Isopycnic Coordinate Ocean Model. , 2006, , .		3
323	Differential regulation of neutrophil chemotaxis to IL-8 and fMLP by GM-CSF: lack of direct effect of oestradiol. Immunology, 2006, 117, 205-212.	4.4	17
324	Spherical mapping for processing of 3D closed surfaces. Image and Vision Computing, 2006, 24, 743-761.	4.5	123

#	Article	IF	CITATIONS
325	Large-Scale Modeling of Parametric Surfaces Using Spherical Harmonics. , 2006, , .		54
326	A Spatio-Temporal Modeling Method for Shape Representation. , 2006, , .		7
327	Multi-scale Voxel-Based Morphometry Via Weighted Spherical Harmonic Representation. Lecture Notes in Computer Science, 2006, , 36-43.	1.3	5
328	An interactive 3D visualization and manipulation tool for effective assessment of angiogenesis and arteriogenesis using computed tomographic angiography. , 2005, 5744, 848.		1
329	Functional analysis of cardiac MR images using SPHARM modeling. , 2005, , .		8
330	A clustering-based approach for prediction of cardiac resynchronization therapy. , 2005, , .		2
331	Modeling Time-Intensity Profiles for Pulmonary Nodules in MR Images. , 2005, 2005, 1359-62.		1
332	Surface Alignment of 3D Spherical Harmonic Models: Application to Cardiac MRI Analysis. Lecture Notes in Computer Science, 2005, 8, 67-74.	1.3	37
333	A Prediction Framework for Cardiac Resynchronization Therapy Via 4D Cardiac Motion Analysis. Lecture Notes in Computer Science, 2005, 8, 704-711.	1.3	5
334	Clustering Based Cardiac Resynchronization Therapy Prediction using Open Source Toolkit PRTools. The Insight Journal, 2005, , .	0.2	0
335	A surface-based approach for classification of 3D neuroanatomic structures. Intelligent Data Analysis, 2004, 8, 519-542.	0.9	86
336	Spherical parameterization for 3D surface analysis in volumetric images. , 2004, , .		1
337	Synergy between IL-8 and GM–CSF in reproductive tract epithelial cell secretions promotes enhanced neutrophil chemotaxis. Cellular Immunology, 2004, 230, 23-32.	3.0	34
338	Shape-based discriminative analysis of combined bilateral hippocampi using multiple object alignment. , 2004, 5370, 283.		4
339	Principal components analysis of hippocampal shape in schizophrenia. Schizophrenia Research, 2003, 60, 206.	2.0	6
340	Morphometric Analysis of Brain Structures for Improved Discrimination. Lecture Notes in Computer Science, 2003, , 513-520.	1.3	6
341	Hippocampal shape analysis: surface-based representation and classification. , 2003, 5032, 253.		41
342	Fast Association Discovery in Derivative Transaction Collections. Knowledge and Information Systems, 2000, 2, 147-160.	3.2	0

#	Article	IF	CITATIONS
343	New algorithms for efficient mining of association rules. Information Sciences, 1999, 118, 251-268.	6.9	31
344	Glu227>Lys substitution in the acidic loop of major histocompatibility complex class I alpha 3 domain distinguishes low avidity CD8 coreceptor and avidity-enhanced CD8 accessory functions Journal of Experimental Medicine, 1996, 184, 1671-1683.	8.5	19
345	Differential ability of isolated H-2 Kb subsets to serve as TCR ligands for allo-specific CTL clones: potential role for N-linked glycosylation Journal of Experimental Medicine, 1995, 181, 1773-1783.	8.5	15
346	Unaggregated serum IgA binds to neutrophil FcαR at physiological concentrations and is endocytosed but cross-linking is necessary to elicit a respiratory burst. Journal of Leukocyte Biology, 1994, 56, 481-487.	3.3	23
347	Lipopolysaccharide and cytokine augmentation of human monocyte IgA receptor expression and function. Journal of Immunology, 1994, 152, 4080-6.	0.8	34
348	Recombinant soluble IgA Fc receptor: generation, biochemical characterization, and functional analysis of the recombinant protein. Journal of Leukocyte Biology, 1993, 53, 223-232.	3.3	13
349	A monoclonal antibody specific for immunoglobulin A receptor triggers polymorphonuclear neutrophil superoxide release. Journal of Leukocyte Biology, 1992, 51, 373-378.	3.3	23
350	Monocyte superoxide secretion triggered by human IgA. Immunology, 1989, 68, 491-6.	4.4	23
351	My 43, a monoclonal antibody that reacts with human myeloid cells inhibits monocyte IgA binding and triggers function. Journal of Immunology, 1989, 143, 4117-22.	0.8	51
352	A combined structural-functional classification of schizophrenia using hippocampal volume plus fMRI activation. , 0, , .		9
353	A system framework for the integration and analysis of multi-modal spatiotemporal data streams: a case study in MS lesion analysis. , 0, , .		1
354	A spatio-temporal multi-modal data management and analysis environment for tracking MS lesions. , 0, , .		0
355	SCENS: a system for the mediated sharing of sensitive data. , 0, , .		0
356	K-means+ Method for Improving Gene Selection for Classification of Microarray Data. , 0, , .		1